

# Aerodynamic Performance Evaluation of a Wind Turbine Blade by Computational and Experimental Method

Irshadhussain I. Master  
M.Tech. Student,  
Department of  
Mechanical Engineering,  
Patel College of Science  
and Technology,  
Rajiv Gandhi Proudयोगiki  
Vishwavidyalaya,  
Ratibad, Bhopal – 462036  
India.

Azim Aijaz Mohammad  
Asst. Professor,  
Department of  
Mechanical Engineering,  
Patel College of Science  
and Technology,  
Rajiv Gandhi Proudयोगiki  
Vishwavidyalaya,  
Ratibad, Bhopal – 462036  
India.

Ratnesh T. Parmar  
Asst. Professor,  
Department of,  
Mechanical Engineering,  
Babaria Inst. Of Tech,  
Vadodara, Gujarat,  
India.

**Abstract--Lift and Drag forces along with the angle of attack are the important parameters in a wind turbine system. These parameters decide the efficiency of the wind turbine. In this paper an attempt is made to study the Lift and Drag forces in a wind turbine blade at various sections and the effect of angle of attack on these forces. In this paper NACA 4420 airfoil profile is considered for analysis of wind turbine blade. The wind turbine blade is modelled and several sections are created from root to tip. The Lift and Drag forces are calculated at different sections for angle of attack from  $0^\circ$  to  $20^\circ$  for low Reynolds number. The analysis showed that angle of attack of  $6^\circ$  has high Lift/Drag ratio. The CFD analysis is also carried out at various sections of blade at different angle of attack. The pressure and velocity distributions are also plotted. The airfoil NACA 4420 is analyzed based on computational fluid dynamics to identify its suitability for its application on wind turbine blades and good agreement is made between results.**

## 1. INTRODUCTION

Wind energy is an abundant resource in comparison with other renewable resources. Moreover, unlike the solar energy, the utilization could not be affected by the climate and weather. Wind turbine invented by engineers in order to extract the energy from the wind. Because the energy in the wind is converted to electric energy, the machine also called wind generator. A wind turbine consists of several main parts, i.e., the rotor, generator, driven chain, control system and so on. The rotor is driven by the wind and rotates at pre-defined speed in terms of the wind speed, so that the generator can produce electric energy output under the regulation of the control system. In order to extract the maximum kinetic energy from wind, researcher put much effort on the design of effective blade geometry. In the early stage, the airfoil of helicopters were used in 2 wind turbine blade design, but now, many specialized airfoils have been invented and used for wind turbine blade design.

Moreover, a rotor blade may have different airfoil in different sections in order to improve the efficiency, so that modern blade is more complicated and efficient comparing to early wind turbine blades. In my early stage, the research on wind turbine blade design was limited on theoretical study. Field testing and wind tunnel testing which need a lot of effort and resources. Due to the development of computer aided design codes, they provide another way to design and analyze the wind turbine blades. Aerodynamic performance of wind turbine blades can be analyzed using computational fluid dynamics (CFD), which is one of the branches of fluid dynamics that uses numerical methods and algorithm to solve to solve and analyze problems of fluid flow. Meanwhile, finite element method (FEM) can use for the blade structure analysis. Comparing to traditional theoretical and experimental methods, numerical method saves money and time for the performance analysis of optimal design of wind turbine blades.

H.V.Mahawadiwar et al [1] carried out Computational Fluid Dynamics (CFD) analysis of wind turbine blade with complete drawing and details of sub-system. The blade material is Cedar wood, strong and light weight. CAD model of the blade profile using Pro-E software is created and the flow analysis of the wind turbine blade mesh is created in the GAMBIT software. CFD analysis of the wind turbine blade is carried out in the FLUENT software. Form this study they conclude as following:

1. Value of numerical power increases as angle of attack increases from  $0^\circ$  to  $7^\circ$ , after  $7^\circ$  the value of numerical power reduced. Hence critical angle of attack for this blade is  $7^\circ$ .
2. The maximum value of coefficient of performance ( $C_{pmax} = 0.271$ ) was saw at angle of attack  $7^\circ$  and at velocity of air 8 m/s.
3. This blade can generate maximum power of 620 W at maximum  $C_p$ , angle of attack  $7^\circ$  and velocity of air 8 m/s.

Chris Kaminsky, Austin Filush, Paul Kasprzak and Wael Mokhtar [2] carried out the work of a VAWT using the NAC A0012-34 airfoil. The system was modelled in Solid Works. They are use of the STAR CCM software to CFD analyzes the air flow around a vertical axis wind turbine to perform. Analysis has been done in three ways as show:

1. To determine CFD analysis analyzed the 2D flow over the chosen airfoil.
2. Determine the analysis looked at the flow over a 3D representation of the airfoil.

3. Finally, a full VAWT assembly was created and analyzed at various wind directions at the  
The airfoil then the 2D and 3D simulations used different angles of attack (0 to 15 degrees) and speeds (15 & 30 mph) to determine. The full assembly included 3 airfoils that were attached into a 5ft high, 3 ft diameter structure. The results of this research on the NACA 001234 airfoil showed it could be a very viable choice for a residential VAWT. The 2D analysis gave a stall angle of about  $8^\circ$ , however, the 3D analysis, it being more accurate, did not provide us with a stall angle. The results for the 3D full assembly analysis of vertical axis wind turbine were incomplete.

C. Rajendran, G. Madhu, P. S. Tide et al [3] had carried out the potential of an incompressible Navier–Stokes CFD method for the analysis of horizontal axis wind turbines. The CFD results are validated against experimental data of the NREL power performance testing activities. Comparisons are shown for the surface pressure distributions at several conditions are show as under taken:

- a) Wind Velocity is 12.5m/s.
- b) Yaw Angle is  $0^\circ$ .
- c) Rotational Speed is 25 rpm.
- d) Turbulence Model is  $k-\omega$  SST.

David Hartwanger et al [4] have aims to develop a practical engineering methodology for the CFD-based assessment of multiple turbine installations. They are constructs the 2D experimental model of wind turbine which is of NREL S809 aerofoil series and compared. Their results with 3D CFD model in XFOIL 6.3 codes and two ANSYS CFX 11.0 versions. It creates the cylindrical domain whose radius  $2L$  and length  $5L$  where  $L$  = turbine radius. For grid generation uses ICEM-CFD (ANSYS) software. In analysis it use  $k-\omega$  turbulence model. There are two main aims for doing analysis is as under show:

1. The primary aim is to predict the lift and drag for 2D experimental wind turbine.
2. Its secondary aim is to compare the results of Lower CFD Fidelity to Higher CFD Fidelity model.

These two aims fulfil with one boundary condition which is use pressure as an inlet condition. The validation of CFD against 2D blade sections showed that the CFD and XFOIL panel code over-predict peak lift and tend to underestimate stalled flow.

The 3D results compared well with experiment over four operating conditions. Results from the 3D corresponding calculated torque output showed good agreement with the 3D CFD model and experimental data. However, for high wind cases the actuator model tended to diverge from the CFD results and experiment.

Hansen and Butterfield [5] discussing recent research conducted regarding the aerodynamics of wind turbines. HAWT blades are made up of varying airfoil cross sections. Depending on the distance from the turbine hub, the airfoil's thickness may change. When close to the hub, rotational velocity becomes less significant and the blade cross section uses a high thickness for structural stability. Close to the edge of the rotor, a much thinner airfoil is used to provide a high lift-drag ratio in the larger rotational velocity area. In many turbines designed and operated during the 1970s and 1980s, aviation airfoils were used, due to their high lift coefficients. However, continued operation of these airfoils highlighted potential drawbacks when applied to wind turbines. Because of the failures of stall-controlled aviation airfoils to adapt to varying wind conditions, airfoil selection and design became a critical focus of wind turbine research.

Gómez-Iradi, et al [6] A new CFD technique for the analysis of HAWTs was developed and validated. The initial premise for this study was to examine the flow compressibility near the tip of wind turbine blades. Due to this flow compressibility, wind turbines often have changed performance and operate closer to stall conditions.

In this study, the geometry was designed using the National Renewable Energy Laboratory (NREL) S809 wind turbine airfoil from 25% of blade span to the blade tip. The solver developed was based upon a second order implicit numerical method with a sliding mesh to account for the relative rotation of the rotor and stationary sections of the turbine. When compared with experimental results from a wind tunnel test, all of the major flow physics, including root and tip vortices, simulated within the project showed qualitative agreement.

R.S. Amano, et. al. [7] carried out most blades available for commercial grade wind turbine incorporated a straight span wise profile and airfoil shaped cross-section. This paper explores the possibility of increasing the efficiency of blades at higher wind speeds while maintaining efficiency at lower wind speed. The blades will be made more efficient at higher wind speed by implementing a swept blade profile. This paper explores two methods for optimizing blade for operation where wind speeds average 7 m/s. The two methods of optimization that are investigated are first, the straight edge blade optimizes the angle of attack and chord length for a given airfoil cross-section at different position along the blade and second implements a swept blade profile. The following conclusion obtained from the research paper. It was observed that swept edge geometry maintains the maximum efficiency at lower oncoming wind speed and delays the stall point resulting in an increase in power at higher oncoming wind speed.

Kentaro hayashi, et. al. [8] carried out Noise reduction of wind turbines has recently become more important due to increasing Largescale turbine developments, stringent noise regulations, and installation of wind farms near residential areas. Wind turbine noise is mainly caused by broadband noise from the blades and can be reduced using noise prediction technologies. Mitsubishi Heavy Industries, Ltd. (MHI) has developed a new method to predict blade noise based on a computational fluid dynamics (CFD) approach and an empirical formula. This method can be used during

the preliminary blade design and has been validated using an actual model. In this report, we present a less noisy blade that was developed by applying this approach at the design stage.

Horia DUMITRESCU, et. al. [9] carried out In this paper two methods for determining the angle of attack on rotating blade from velocity and pressure measurement are presented. To derive the lift and drag coefficients an angle of attack is required in combination with the normal and tangential force coefficients. A proper inflow angle of attack is not directly available and two simple methods have been proposed to compute correctly the angle of attack for wind turbines. The first method using the measured/ computed velocities requires an iterative calculation, while the second technique using measured/computed pressures no iteration is required and the monitor points can be chosen to be closer to the blade 18 surface. On the other hand, the difficulty of using the pressure-method is to find the separation point where the local circulation changes sign and the distribution of skin friction should be determined from CFD solutions. Therefore, how to determine the effective angle of attack is a key factor to understand the stall flow.

S. RAJAKUMAR, et. al. [10] carried out In this paper an attempt is made to study the Lift and Drag forces in a wind turbine blade at various sections and the effect of angle of attack on these forces. In this paper NACA 4420 airfoil profile is considered for analysis of wind turbine blade. The Lift and Drag forces are calculated at different sections for angle of attack from 0 to 12 for low Reynolds number. The analysis showed that angle of attack of 5 has high Lift/Drag ratio.

Horia DUMITRESCU, et. al. [11] carried out the short separation bubbles which form near the leading edge of the inboard sections of the blade prior to the onset of leading edge stall have been analyzed in detail, including some effects of viscous inviscid interaction. The transition point is assumed to correspond to the minimum skin friction. The momentum integral technique for the wind turbine blade boundary layer has been extended to include the separated and reattaching shear layer in a leading- edge bubble of a wind turbine blade For cases where separated areas exist, a classical boundary layer approach is in principle no more valid (normal pressure gradient, formation of vortices, etc.). However, provided the flow is not widely separated, good description of the viscous effects is obtained, using inviscid flow calculation input. Based on the described boundary layer method, the physical processes which influence the inboard stall-delay phenomenon have been explained, including the onset of the three-dimensional effects and the increase of the lift coefficients.

Aravind Lovelin [12] carried out In this paper a Horizontal axis wind turbine blade profile NACA 63-415 is analyzed for various angles of attack. The coefficient of Lift and drag is calculated for this NACA 63-415 for various angles of attack from 0° to 16° and the maximum ratio is achieved at 2° of angle of attack. The coefficient of Lift increases with increase in angle of attack up to 8°. After 8°, the coefficient of lift decreases and stall begins to occur. The drag force begin of dominate beyond this angle of attack. The rate of increase in lift is more for angle of attack

from 0° to 8° and then it starts to decrease. The drag increase gradually until 5° angle of attack and then rapidly increases. The CFD analysis is carried out using STAR-CCM+ software. These results are compared with the wind tunnel experimental values for validation.

Ryoichi Samuel et. al. [13] carried out this paper explores the possibility increasing the number of profitable sites by optimizing wind turbine blade design for low wind speed areas. Wind turbine blade profiles are often constructed using the Blade Element Momentum theory (BEM). This theory will produce the angle of twist and chord length for a given airfoil cross section and rotation speed at a finite number of positions along the span of the blade. From these two dimensional sections a three dimensional shape can be extruded. The BEM theory accomplishes this by treating a given cross section as an independent airfoil which processes wind with a speed and direction that is a vector sum of the oncoming wind and the wind generated by rotation. Since the direction and magnitude of the 20 wind generated by rotation changes as a function of span wise position, so too must the airfoil cross section. The BEM theory is not entirely accurate if the data for the airfoil cross sections that are used have not been corrected for rotational motion. It is for this reason that CFD analysis is necessary for new blade designs.

## 2. LIFT AND DRAG

Lift on a body is defined as the force on the body in a direction normal to the flow direction. Lift will only be present if the fluid incorporates a circulatory flow about the body such as that which exists about a spinning cylinder. The velocity above the body is increased and so the static pressure is reduced. The velocity beneath is slowed down, giving an increase in static pressure. So, there is a normal force upwards called the lift force.

The drag on a body in an oncoming flow is defined as the force on the body in a direction parallel to the flow direction. For a windmill to operate efficiently the lift force should be high and drag force should be low. For small angles of attack, lift force is high and drag force is low. If the angles of attack ( $\alpha$ ) increases beyond a certain value, the lift force decreases and the drag force increases. So, the angle of attack plays a vital role.

## 3. METHOD OF ANALYSIS

The aerofoil NACA 4420 is chosen for blade modeling as shown in Fig.1.

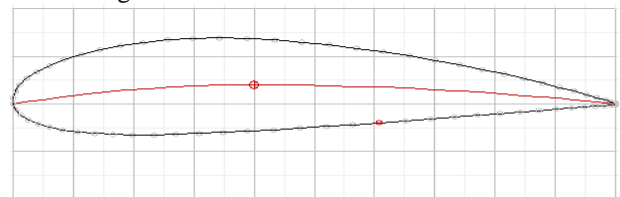


Fig.1. NACA 4420 Airfoil

NACA 4420 profiles are obtained from Design Foil Workshop for various chords. The modeling is done with

Solid Works. The blade is modelled for the specification given in Table1

Profile	NACA 4420
Root chord length	1651 mm
Tip chord length	650 mm
Length of blade	10700 mm
Hub diameter	337.5 mm
Hub length	1465 mm
Hub to blade(neck)	1475 mm

Table1. Blade specification

The velocity triangle of airfoil profile is used to calculate lift and drag forces shown in Fig.2.

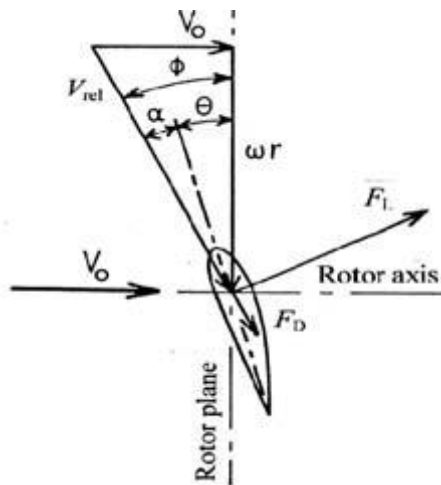


Fig.2 Blade velocity triangle

The value of φ is found by the following formula. The wind velocity is taken as 8m/s and the speed is taken as 45 r.p.m.

$$\phi = \tan^{-1} (8 / (2\pi r (45/60)))$$

The angle of attack (AOA) α is found by the following formula

$$\alpha = \phi - \theta$$

The angle of attack value is given as input in the Design Foil Workshop software and the values of CL and CD are found out.

The lift and drag forces are calculated by the following formula and the lift to drag ratio (L/D ratio) is also found out.

$$\text{Lift} = (1/2) \cdot \rho \cdot C_L \cdot c \cdot L \cdot V_{rel}^2$$

$$\text{Drag} = (1/2) \cdot \rho \cdot C_D \cdot c \cdot L \cdot V_{rel}^2$$

Where ρ – density of air - 1.225 kg/m<sup>3</sup>

c – Chord length in meter – 1m

L – Length of the blade element - 1m

Vrel – relative velocity of air in m/s

$$= ((V_o)^2 + (\omega r)^2)^{0.5}$$

The values of CL and CD were found out for various angles of attack.

$$\text{Lift} = (0.5 \cdot \rho \cdot c \cdot L \cdot C_L \cdot V_{rel}^2)$$

$$\text{Drag} = (0.5 \cdot \rho \cdot c \cdot L \cdot C_D \cdot V_{rel}^2)$$

The Lift and Drag forces are calculated for the angle of attack from 0° to 20°. The Lift/Drag ratio is calculated for different angle of attack ranges from 0° to 20° for the velocity ranges from 5 to 20 m/sec.

Angle of attack	L/D RATIO						
	Vo=5 m/s	Vo=7 m/s	Vo=10 m/s	Vo=12 m/s	Vo=15 m/s	Vo=17 m/s	Vo=20 m/s
0	50.7	53.6	55.6	56.2	57.9	59.1	60.3
1	59.7	62.4	64.7	68.5	69.9	71.3	72.8
2	67.2	70.8	73.5	73.0	75.8	78.0	80.4
3	70.0	73.0	76.3	80.6	82.2	84.7	86.5
4	75.4	78.7	78.8	83.9	86.3	88.0	88.1
5	<b>74.3</b>	77.8	<b>81.1</b>	82.6	84.9	85.7	88.0
6	72.3	<b>75.5</b>	78.4	<b>83.6</b>	<b>85.0</b>	83.2	<b>85.3</b>
7	69.2	72.5	75.1	79.7	81.5	<b>83.5</b>	85.0
8	65.8	68.7	71.4	75.5	77.1	78.8	80.1
9	64.4	64.5	66.8	70.7	72.1	74.0	75.1
10	59.6	62.2	61.6	65.2	66.7	68.0	69.3
11	54.6	56.7	58.8	61.9	63.4	64.8	63.6
12	49.7	51.6	53.3	56.2	57.5	58.7	59.7
13	52.5	58.4	67.1	73.8	82.5	86.5	97.7
14	49.6	55.7	64.8	72.0	80.9	84.3	96.8
15	46.8	53.1	62.5	69.3	79.4	82.4	95.9

Table2. Lift/Drag Ratio

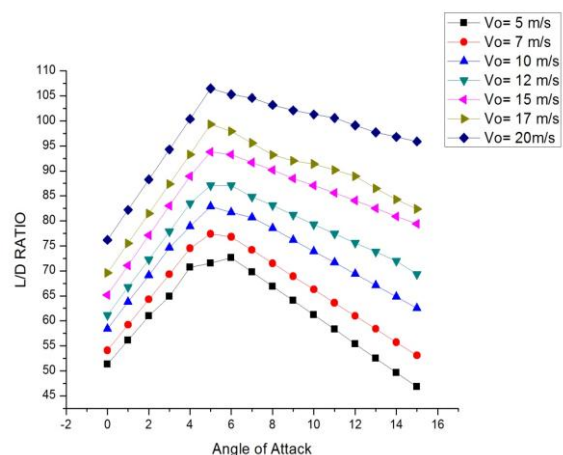


Fig.3. Correlation between L/D ratio and angle of attack



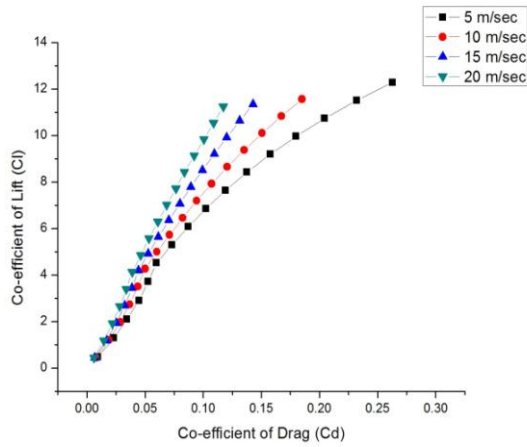


Fig.4. Correlation between  $C_L$  and  $C_D$

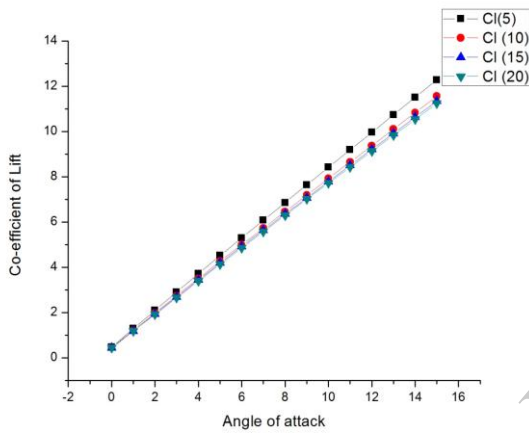


Fig.5. Increase in lift for various Angle of Attack

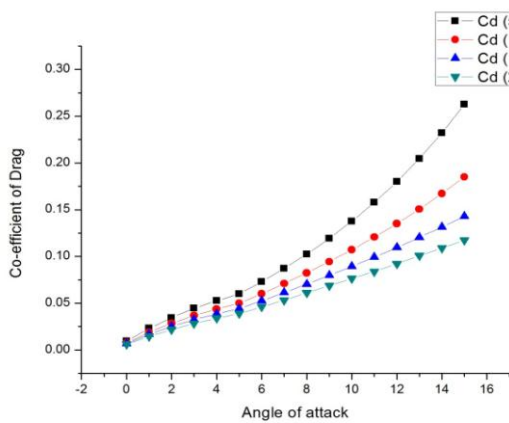


Fig.6 Increase in Drag for various Angle of Attack

### 5.4 Comparison of the Analysis Methods:

At the velocity 5 m/s

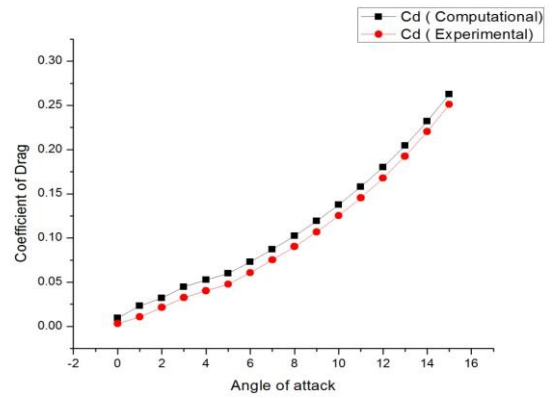


Fig.7 Coefficient of Drag ( $C_D$ ) versus Angle of attack

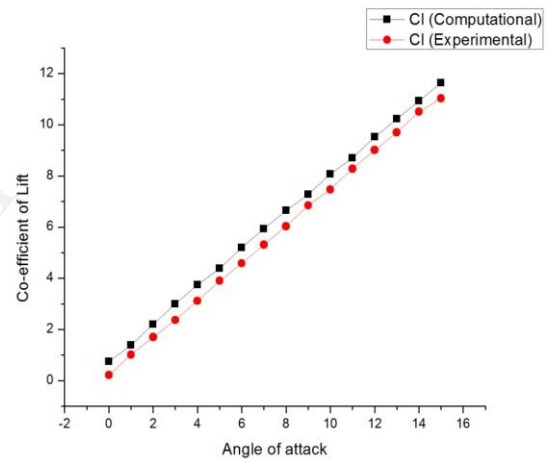


Fig.8 Coefficient of Lift ( $C_L$ ) versus Angle of attack  
At the velocity 10 m/s

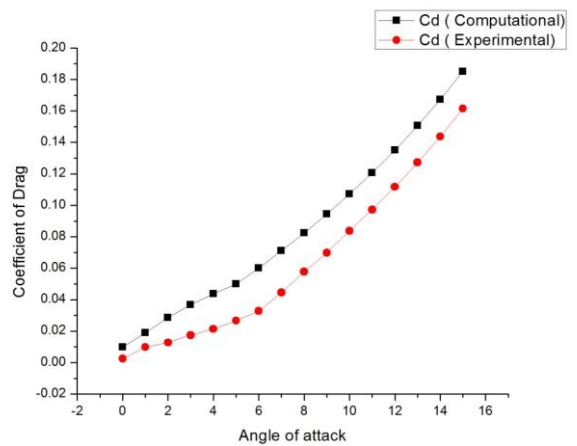


Fig.9 Coefficient of Drag ( $C_D$ ) versus Angle of attack

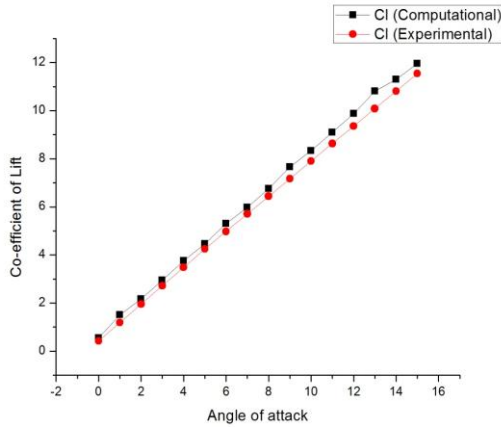


Fig.10 Coefficient of Lift ( $C_L$ ) versus Angle of attack

**At the velocity 15 m/s**

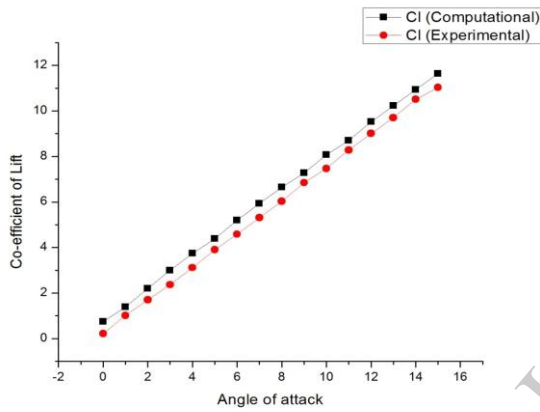


Fig.11 Coefficient of Drag ( $C_D$ ) versus Angle of attack

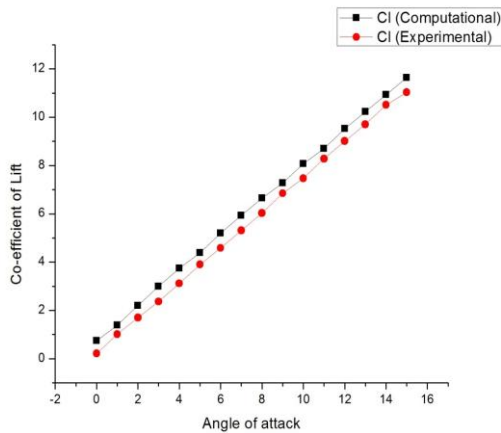


Fig.12 Coefficient of Lift ( $C_L$ ) versus Angle of attack

**4. NUMERICAL METHOD**

The numerical method utilized for the simulation had a density based solver with implicit formulation, 2-D domain geometry, absolute velocity formulation, and superficial

velocity for porous formulation. For this test, a simple solver and an external compressible flow model for the laminar was utilized. The green-gauss cell based was used for the gradient option. There are different equations used for flow, laminar, species, and energy. A simple method was used for the pressure-velocity coupling. For the discretization, a standard pressure was used, and density, momentum and turbulent kinetic energy were set to second order upwind.

**4.1. Flow Analysis**

The computational flow analysis is also performed for NACA 4420 profile. The four sections are considered for flow analysis at the blade from root to tip show in Table.3.

Section	Distance from hub (m)	Chord length (m)
1	2.95	1.651
2	5.275	1.348
3	8.375	0.9469
4	10.7	0.65

**Table 3. Sections from hub**

The maximum L/D ratio is achieved at 6° of angle of attack, for the average velocity of 20 m/sec. Hence the 2-D airfoil sections are created for analysis in ANSYS FLUENT. The aerofoil profile with specific boundary is created in Creo and the computational flow analysis is performed in ANSYS FLUENT. A smart fine mesh is created for the flow area.

**4.2. Geometry and Boundary conditions**

Inlet velocity for the experiments and simulations is 10 m/sec. A fully laminar flow solution was used in ANSYS FLUENT, where linear laminar equations were used. A simple solver was utilized and the operating pressure was set to zero. Calculations were done for the “linear” region, i.e. for angles of attack 5 degrees, due to greater reliability of both experimental and computed values in this region. The airfoil profile and boundary conditions are all created.

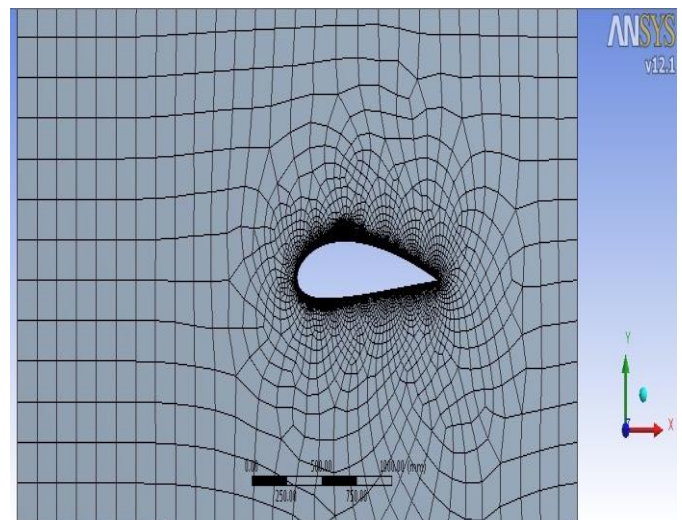


Fig.13 Meshing

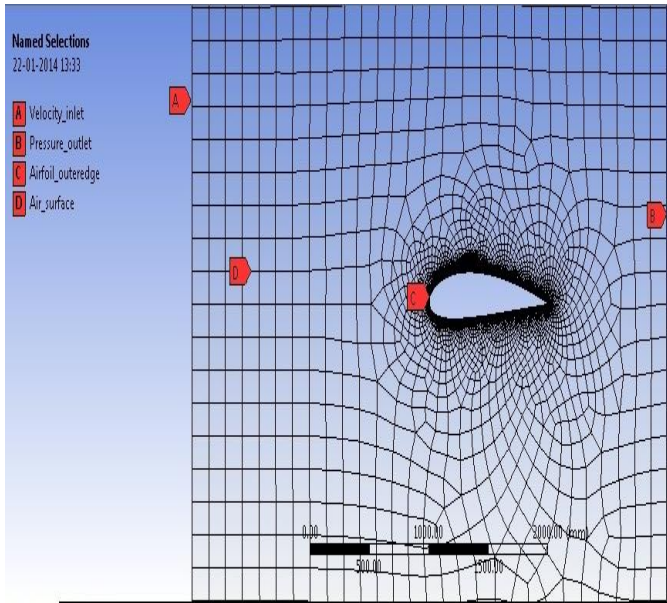


Fig.14 Geometry with boundary condition

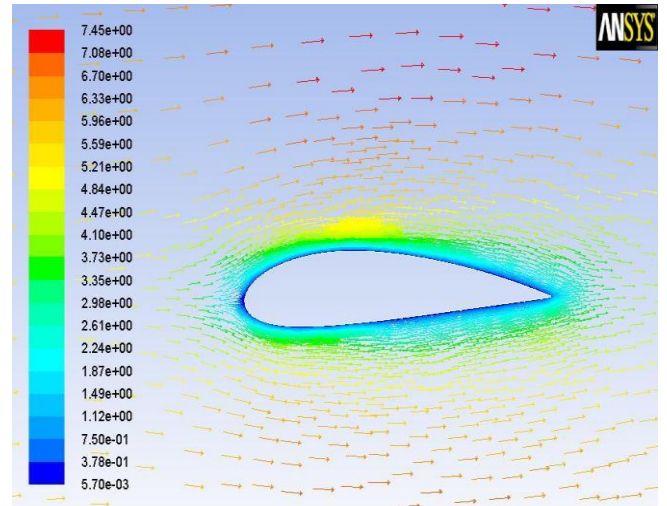


Fig.17 Velocity Plot – 5° Angle of attack

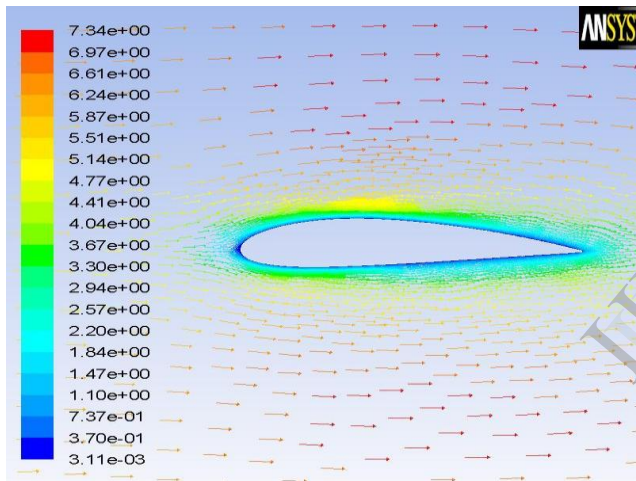


Fig.15 Velocity Plot – 0° Angle of attack

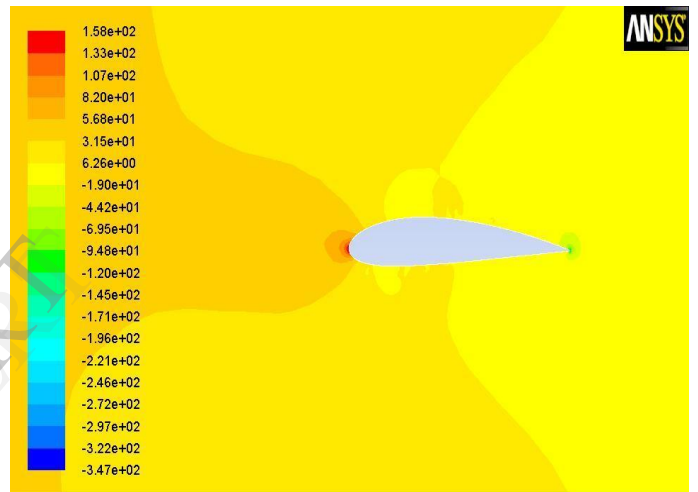


Fig.18 Pressure Plot – 5° Angle of attack

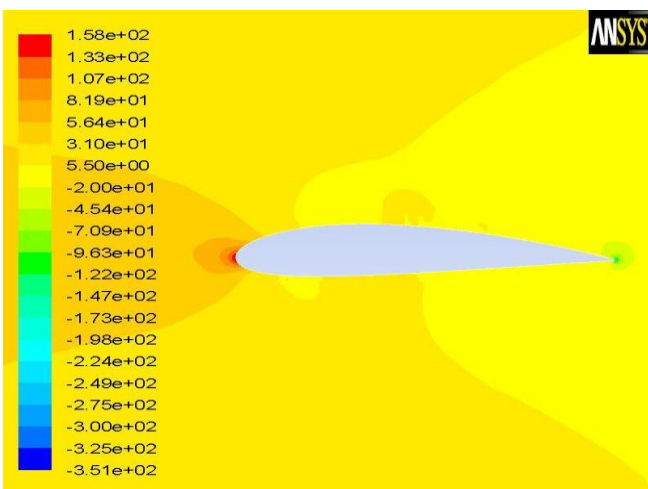


Fig.16 Pressure Plot – 0° Angle of attack

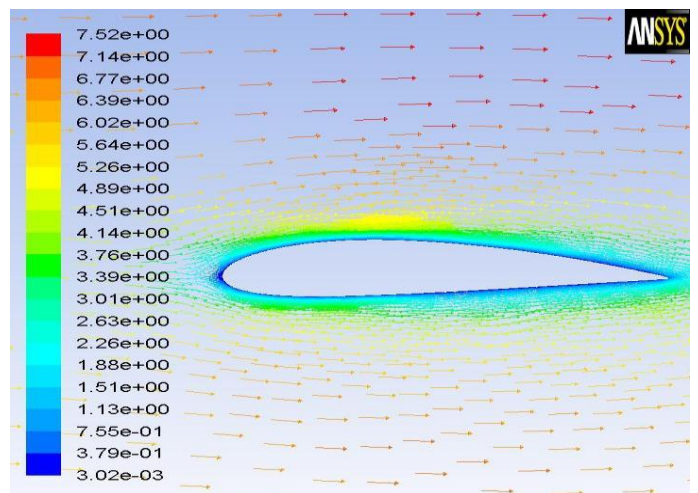


Fig.19 Velocity Plot – 10° Angle of attack



## 5. RESULTS AND DISCUSSION

In this paper a Horizontal axis wind turbine blade with NACA 4420 is designed and analysed for different angle of attack and at various sections.

The blade with constant angle of attack throughout the length is analyzed to find the maximum L/D ratio. This is done at angle of attack ranging from  $0^\circ$  to  $15^\circ$  for the velocity varies from 5 -20 m/sec. The maximum L/D ratio is achieved at  $6^\circ$  of angle of attack, for the average velocity of 20 m/sec. It is found that blade with  $6^\circ$  angle of attack has the maximum L/D ratio.

The coefficient of Lift and drag is calculated for this NACA 4420 series for the angle of attack  $0^\circ$  to  $20^\circ$ . The coefficient of Lift increases with increase in Angle of attack up to  $15^\circ$ . After  $15^\circ$ , the coefficient of lift decreases and stall occurs at this angle of attack.

The lift force at various lengths from hub to tip is analyzed and it is cleared that lift force increases from hub to tip for all range of angle of attack. The lift force increases with increase in angle of attack up to  $14^\circ$  and it starts to decrease after  $14^\circ$ . The drag force begin of dominate beyond this angle of attack. The rate of increase in lift is more for angle of attack from  $0^\circ$  to  $10^\circ$  and between  $10^\circ$  to  $15^\circ$  the rise in lift force is less.

But the drag force increases with increase in angle of attack from hub to tip. The rate of increase in drag increase gradually unlike the rate of increase in lift from  $0^\circ$  to  $16^\circ$  of angle of attack and between  $10^\circ$  to  $15^\circ$  the rise in lift force is less.

The CFD analysis also carried out using ANSYS FLUENT software. The velocity and pressure distribution at various angles of attack of the blade is shown in Fig. 15-22. These results are coinciding with the wind tunnel experimental values. Hence the results are validated with the experimental work is shown in Fig.7-12.

The results demonstrate the pressure distribution over the airfoil. The pressure on the lower surface of the airfoil is greater than that of the incoming flow stream and as a result of that it effectively pushes the airfoil upward, normal to the incoming flow stream. On the other hand, the components of the pressure distribution parallel to the incoming flow stream tend to slow the velocity of the incoming flow relative to the airfoil, as do the viscous stresses.

It could be observed that the upper surface on the airfoil experiences a higher velocity compared to the lower surface. By increasing the velocity at higher Mach numbers there would be a shock wave on the upper surface that could cause discontinuity.

## ACKNOWLEDGEMENT

The authors wish to thank Maharaja Sayajirao University of Baroda, Kalabhavan, Baroda, Gujarat, India for granting permission to carry out this work. The valuable suggestions of Prof. Arvind Mohite, is gratefully acknowledged.



Fig.20 Pressure Plot – $10^\circ$  Angle of attack

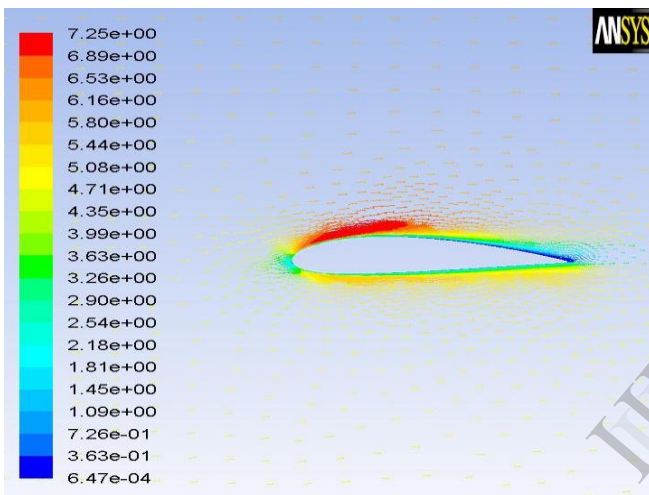


Fig.21 Velocity Plot –  $15^\circ$  Angle of attack

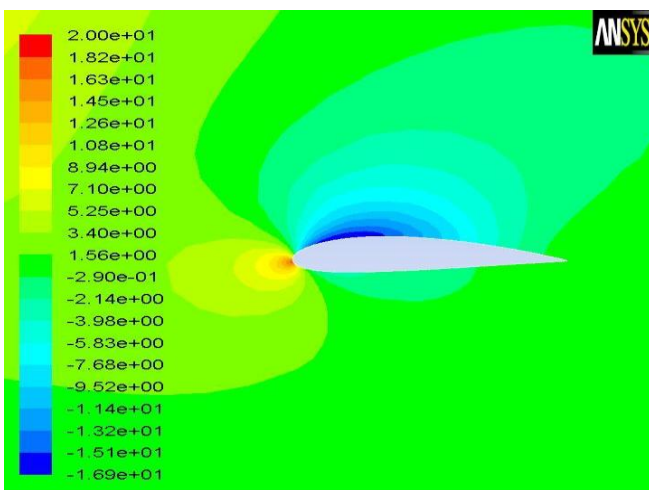


Fig.22 Pressure Plot –  $15^\circ$  Angle of attack



## REFERENCES

- [1] H. V. Mahawadiwar, V.D. Dhopte, P.S.Thakare, Dr. R. D. Askhedkar, "CFD Analysis of Wind Turbine Blade", International Journal of Engineering Research and Applications, May-Jun 2012, PP- 3188-3194.
- [2] Chris Kaminsky, Austin Filush, Paul Kasprzak and Wael Mokhtar, "A CFD Study of Wind Turbine Aerodynamics", Proceedings of the 2012 ASEE North Central Section Conference
- [3] C. Rajendran, G. Madhu, P.S. Tide, K. Kanthavel, "Aerodynamic Performance Analysis of HAWT Using CFD Technique", European Journal of Scientific Research, ISSN 1450-216X Vol. 65, No. 1 (2011), PP 28-37.
- [4] David Hartwanger and Dr. Andrej Howat, "3D Modelling of a Wind Turbine Using CFD", NAFEMS Conference, 2008.
- [5] Hansen, A. C., and Butterfield, C. P., 1993, "Aerodynamics of Horizontal-Axis Wind Turbines," Annual Review of Fluid Mechanics, 25, pp. 115 - 149.
- [6] Gómez-Iradi, S., Steijl, R., and Barakos, G. N., "Development and Validation of a CFD Technique for the Aerodynamic Analysis of HAWT," Journal of Solar Energy Engineering, 131, (3).
- [7] R.S. Amano, R.J. Malloy "CFD Analysis on Aerodynamic Design Optimization of Wind Turbine Rotor Blade" 2009, m pp. 71-75.
- [8] Kentaro hayashi, Hiroshi nishino, hiroyuki hosoya, koji fukami, Tooru matsuo, takao kuroiwa "low-noise design for wind turbine blades" March-2012, pp-74-77
- [9] Horia dumitrescu, Vladimir cardos florin frunzulica, Alexandru Dumitrache "determination of angle of attack for rotating blades" 2012
- [10] S. Rajakumar, Dr.D.Ravindran "computational fluid dynamics of wind turbine blade at various angles of attack and low Reynolds number" 2010
- [11] Horia dumitrescu, Vladimir cardos "the turbulent boundary Layer on wind turbine blades" 2010 pp-125-136
- [12] Dr. S. P. Vendan, S. Aravind Lovelin, M. Manibharathi and C. Rajkumar "Analysis of a Wind Turbine Blade Profile for Tapping Wind Power at the Regions of Low Wind Speed".
- [13] Ryoichi Samuel Amano and Ryan Malloy "Horizontal Axis Wind Turbine Blade Design" 2009

## Nomenclature

- A - Swept area of rotor
- $\alpha$  - Angle of attack
- $C_D$  - Drag coefficient
- $C_L$  - Lift coefficient
- D - Drag force
- L - Lift force
- N - RPM of the rotor
- P - Power developed by rotor
- r - Radius of rotor
- R - Resultant force acting on aerofoil
- V - Free stream velocity
- $V_T$  - Tangential velocity
- $V_R$  - Resultant Velocity
- $\omega$  - Angular Velocity

## Subscripts

- D - Drag
- L - Lift
- rel - relative